

1 **TITLE:** Sequential scute growth layers reveal developmental histories of hawksbill sea turtles

2 **AUTHORS:** Kyle S. Van Houtan,^{a*} T. Todd Jones,^b Molly E. Hagemann,^c Joel Schumacher,^d
3 George Phocas,^e Alexander R. Gaos,^b and Jeffrey A. Seminoff^d

4 **AFFILIATIONS:** ^a Nicholas School of the Environment, Duke University, Durham, North
5 Carolina 27708 USA; ^b NOAA Fisheries, Pacific Islands Fisheries Science Center, Honolulu,
6 Hawaii 96818 USA; ^c Vertebrate Zoology Collections, Bernice Pauahi Bishop Museum,
7 Honolulu, Hawaii 96817 USA; ^d NOAA Fisheries, Southwest Fisheries Science Center, La Jolla,
8 California 92037 USA; ^e U.S. Fish and Wildlife Service, Office of Law Enforcement, Regional
9 Attaché (ret.) - U.S. Embassy, Bangkok, Thailand.

10 * Send correspondence to: kyle.vanhoutan@gmail.com

11 **KEY WORDS:** highly migratory species, biogeography, sclerochronology, population structure,
12 ontogenetic shifts

13 **ABSTRACT WORD COUNT:** 198

14 **TEXT WORD COUNT:** 4,803

15 **No. FIGURES:** 5

16 **No. REFERENCES:** 66

17 **SUPPLEMENT:** 2 tables & 1 figure

18
19
20
21
22
23
24
25
26
27
28 **ABSTRACT**

29 Understanding the basic life history patterns of highly migratory species is important for effective
30 management. For sea turtles, evidence of developmental biogeography and discrete life stage
31 residency provides key information for understanding resource use and population threats and
32 defining conservation priorities. Resolving these knowledge gaps is not straightforward, however.
33 Inaccessible habitats, low survivorship, late maturity ages, and technology limitations all
34 complicate monitoring individuals continuously throughout their life span. Here we expand on
35 previous studies and document a near-complete tissue record in the ultimate posterior marginal
36 scutes of hawksbill sea turtle (*Eretmochelys imbricata*) carapace. Stable isotope analysis (SIA) of
37 ventral scute surfaces reveals differences between 3 geographically isolated populations in the
38 Pacific and Atlantic basins. Additionally, sequential sampling and SIA along growth line contours
39 of sectioned scutes reveals developmental movements. Perhaps surprisingly, no clear or general
40 patterns emerge. Bivariate isoscape data (stable carbon, $\delta^{13}\text{C}$, and nitrogen $\delta^{15}\text{N}$) indicate only 1
41 of 6 Central Pacific hawksbills showed a distinct ontogenetic shift. And while all 3 Western
42 Pacific individuals showed evidence of ontogenetic shifts, these individuals had 3 unique
43 patterns. We summarize regional stable isotope values for common hawksbill foraging items,
44 discuss drivers of regional nitrogen structure, and make recommendations for future study.

45 INTRODUCTION

46 Stable isotope analysis (SIA) is a relatively low-cost diagnostic tool for inferring individual-based
47 ecological information from marine consumers. Isotopic compositions of animal tissues integrate
48 ecosystem and foraging information (Deniro and Epstein 1981; Popp et al. 2007), and thus, when
49 an animal moves among geographically discrete food webs the stable isotope values of its tissues
50 reflect these habitat shifts (Reich et al. 2007; Hobson and Wassenaar 2008; Ramirez et al. 2015).
51 Known as stable isotope tracking, this method carries some advantages over traditional
52 population monitoring via mark-recapture or biotelemetry tracking. One, SIA does not require an
53 initial marking of individuals to obtain subsequent data but provides information on prior
54 experiences. Two, if the sampled tissues provide a developed chronology, then SIA may provide
55 a time series and not simply a snapshot of ecological information (Becker et al. 1991; Grottoli
56 and Eakin 2007; Trueman et al. 2012). Three, unlike most biotelemetry studies that focus on
57 geographic locations, SIA also has the potential to reveal foraging niche and trophic position
58 (Seminoff et al. 2012; Clyde-Brockway et al. 2022). Four, SIA and other diagnostic tools can be
59 applied to both living organisms and dead tissues, and therefore may access natural history
60 archives to expand sample sizes and derive novel historical records (Gagné et al. 2018b; Miller et
61 al. 2020).

62 As distinct isotopic patterns have been described across marine regions (“isoscapes”),
63 stable isotope tracking has been broadly applied to understand the life history of sea turtles.
64 Researchers have analyzed soft high-turnover tissues like skin and blood (Seminoff et al. 2006;
65 Seminoff et al. 2012; Wedemeyer-Strombel et al. 2021; Clyde-Brockway et al. 2022), as well as
66 hard tissues with sequential layering like scute and bone (Reich et al. 2007; Avens et al. 2013;
67 Van Houtan et al. 2016a; Turner Tomaszewicz et al. 2017). When time-specific growth layers in
68 these hard tissues are serially sampled, researchers can measure isotope values across an
69 organism’s distinct life stages. Pioneering work by Reich et al. (2007) performed SIA of keratin
70 plugs of old and new scute tissues from green turtles (*Chelonia mydas*) in the western North
71 Atlantic to reveal a transition from oceanic to neritic habitats during early juvenile development.
72 However, Reich et al. (2007) only sampled two points in each individual’s life history, and thus
73 were unable to validate the duration of transition age of these discrete stages. SIA of scute plugs
74 has since been conducted on successive scute growth layers to study habitat use by green and
75 hawksbill (*Eretmochelys imbricata*) turtles (Vander Zanden et al. 2013; Wedemeyer-Strombel
76 et al. 2021), yet without producing a contiguous and complete life history record.

77 SIA has also been examined in the growth layers of humerus bones from loggerhead
78 (*Caretta caretta*), Kemp’s ridley (*Lepidochelys kempii*), green, and hawksbill turtles to document
79 chronologies of habitat use (Avens et al. 2013; Ramirez et al. 2015; Turner Tomaszewicz et al.
80 2017; Avens et al. 2020; Turner Tomaszewicz et al. 2022). While these studies have provided
81 new and important life history insights, one limitation of this approach is that complete life
82 history records are frequently precluded by the loss of early growth layers due to inner bone
83 resorption (Snover 2002; Van Houtan et al. 2014a) or scute sloughing (Caine 1986; Palaniappan
84 2007). An ideal tissue for SIA chronology study in sea turtles would sequentially deposit layers,
85 retain early life stage layers, and provide a full life record. Known as tortoiseshell in international
86 trade (Donnelly 2008; Miller et al. 2019), the robust keratin deposits in hawksbill carapace scutes
87 present a good candidate for study. Van Houtan et al. (2016a) advanced earlier studies of
88 hawksbill carapace scutes (Tucker et al. 2001; Palaniappan 2007) by discovering a near-complete
89 chronology in the ultimate posterior marginal (PM) scutes from hawksbill carapaces, tabulating
90 internal growth lines, and using bomb radiocarbon ($\delta^{14}\text{C}$) to estimate tissue age.

91 Here we expand on previous approaches by examining SIA in the ventral surface of
92 central scutes and internal layers of PMs in hawksbill sea turtles. We first source hawksbill scutes
93 through a variety of pathways and institutional partnerships (see Methods) to obtain scutes from

94 all demographic stages and spanning 4 marine regions. Then, we compare SIA results from the
95 most recently deposited ventral surface keratin tissues to examine patterns across ontogeny within
96 and between geographic regions. Next, we perform SIA on sequential scute growth layers for 6
97 hawksbills from Hawaii and 3 hawksbills from the Western Pacific to reveal details from the
98 cryptic early life history phase. Lastly, we collect stable isotope values and compile published
99 records for common hawksbill forage items across the Pacific as a comparative reference.

100

101 **MATERIALS and METHODS**

102 *Specimen collection*

103 We obtained hawksbill carapace samples from strandings, museum collections, and U.S. federal
104 repositories in accordance with U.S. Endangered Species Act guidelines (U.S. Fish & Wildlife
105 Service permit #TE-72088A-0). Originating institutions provided sample metadata including
106 location of origin, date of death or receipt, morphometrics, and sex. Specimens arrived in a
107 variety of dispositions: whole organisms (frozen, taxidermized), whole carapaces (dried), and
108 disintegrated scutes. Strandings were from NOAA's ongoing sea turtle stranding program at the
109 Pacific Islands Fisheries Science Center in Honolulu, Hawaii (see: Work et al. 2004; Van Houtan
110 et al. 2010; Balazs et al. 2015; Brunson et al. 2022). The Bernice Pauahi Bishop Museum
111 provided samples from their collections and the US Fish & Wildlife Service, Office of Law
112 Enforcement (Clark R. Bavin National Fish and Wildlife Forensics Laboratory, and National
113 Wildlife Property Repository) provided seized specimens. Hatchling scutes came from emerged
114 or partially-emerged, deceased hatchlings during nest excavations on Maui and Hawaii Islands in
115 conjunction with nest monitoring programs (e.g., Seitz et al. 2012; Gaos et al. 2021). Table S1
116 provides more details and metadata on the hawksbill specimens.

117 Hawksbill forage item samples (macroinvertebrates and macroalgae) were derived from
118 field surveys and stranded turtles, and supplemented with additional data from the published
119 literature. Previous nearshore reef surveys collected macroalgae in the Main Hawaiian Islands
120 (Van Houtan et al. 2014b). We supplemented these collections with surveys of established
121 hawksbills foraging sites on Oahu, Maui, and Hawaii islands in 2012-2014, and at Rose Atoll,
122 American Samoa in 2012. During necropsy, we obtained additional undigested forage specimens
123 from the upper gastrointestinal tract (i.e., esophagus) of 2 hawksbills from Kwajalein Atoll,
124 Republic of the Marshall Islands. These turtles died from traumatic injuries in September 1992,
125 were kept in a freezer, and necropsied in July 2012 following established protocols (Work 2000).
126 Published studies provided further isotope values from additional hawksbill forage items
127 collected on Hawaii island in 2007-2008 (Graham 2009) and at Palmyra Atoll in 2008-2010
128 (Kelly 2012).

129 *Specimen preparation and sample extraction*

130 Following published methods (Van Houtan et al. 2016a; Miller et al. 2019) we prepared all
131 hawksbill scute specimens for imaging, microsampling and diagnostic analysis. We began by
132 separating carapace and marginal scutes from their adjoining tissues through natural tissue
133 degradation. This process enclosed carapaces in perforated heavyweight polypropylene bags and
134 submerged them in seawater for < 7 days. Then we removed surface algae, epibionts, debris, and
135 cleaned scute surfaces with tap water and mild detergent. We rinsed the cleaned scutes first with
136 deionized water, then with 90% ETOH and air-dried scutes in a fume hood for 24 hours.
137 Following previous studies (Dailer et al. 2010; Van Houtan et al. 2014b) we rinsed collected
138 macroalgae in deionized water, patted samples dry with cloth towels, and placed them on
139 aluminum foil in a drying oven at 60 °C until fully desiccated (24-48 hours). We repeated this
140 same procedure for additional hawksbill forage items, separating forage items into discrete

141 taxonomic groups.

142 We first sampled superficial scute surfaces as previous studies examined these tissue
143 sections for patterns of growth (Tucker et al. 2001; Palaniappan 2007) and stable isotope content
144 (Reich et al. 2007; Kelly 2012). Using central carapace scutes from Hawaii, Caribbean, and
145 American Samoa specimens, we examined the newest tissue deposits—the center of the ventral
146 side of the scute that directly contacts the living epidermis (see below, also Palaniappan 2007)—
147 to capture a snapshot of their most recent life history and ecosystem experience (Van Houtan et
148 al. 2016a). With a scalpel, we scraped the exterior of ventral scute surfaces, moving perpendicular
149 to the edge of a No. 21 blade (at < 0.5 mm depth) to create 5 mg of sample material. For
150 hatchlings only, as this demographic has no pronounced scute chronology, we shredded whole
151 scutes using medical grade scissors (Excelta® #364, 1.25” blade). Using a ceramic mortar and
152 pestle, we further homogenized all extracted scute and forage item material into a fine powder
153 storing all sample homogenate in 1.5 mL Nalgene™ cryogenic vials for isotope analysis.

154 Seeking a more complete life history record, we supplemented these ventral scute surface
155 samples by revealing and sampling sequential growth layers within posterior marginal (PM)
156 scutes, derived from Western Pacific and Hawaii specimens. Following Van Houtan et al.
157 (2016a), we used a low speed precision cutter (Buehler Isomet™, No. 11-1280-170) with
158 diamond wafering blades (Buehler 15HC, No. 11-4244) to make 1.5 mm thick sagittal cross
159 sections in ultimate PM scutes. To reveal growth layers, we polished the cross sectioned wafers
160 (Buehler ECOMET III™ 800 Polisher, Mark V Laboratory® A/O lapping film) sequentially
161 moving from coarse to finer lapping film. We imaged each polished PM cross section with a
162 brightfield, phase contrast, and darkfield equipped microscope (scope: Olympus BX41™,
163 camera: ImagingPlanet 20MPX™, adapter: Olympus U-TVO.5XC-3, firmware: IMT i-Solution
164 Lite), using software (Adobe Photomerge®) to stitch a single composite image from multiple
165 sub-field image frames (e.g., Fig. 2B). The variable illumination and contrast capabilities of this
166 microscope was useful for identifying growth lines across variously melanized sections of scute
167 keratin.

168 Following (Van Houtan et al. 2016a), we counted the apparent growth lines on each PM
169 composite image and extracted tissue samples with a Carpenter Microsystems CM2
170 microsampling system (Avens et al. 2013; Turner Tomaszewicz et al. 2017). Here, we drilled ~1
171 mm paths along PM growth contours (see Figs. 3-4), extracting > 1.5 mg of keratin powder for
172 each microsample, repeating this process to capture material representing distinct developmental
173 stages in each PM. Further treatment of scute material for lipid extraction was not required due to
174 low C:N ratios among samples (see below; Turner Tomaszewicz et al. 2015).

175 *Isotope Analysis and Data Visualization*

176 We determined bulk $\delta^{13}\text{C}$ and $\delta^{15}\text{N}$ stable isotope compositions using an on-line C-N analyzer
177 coupled with an isotope ratio mass spectrometer (Finnigan ConFlo II/DeltaPlus). Approximately
178 1.0 mg of each sample was loaded into sterilized Sn capsules and analyzed by a continuous-flow
179 isotope-ratio mass spectrometer at the Light Stable Isotope and Mass Spectrometry Laboratory at
180 University of Florida (Gainesville, Florida, USA). We used a Costech ECS 4010 elemental
181 combustion system interfaced via a ConFlo III device (Finnigan MAT) to a DeltaPlus gas
182 isotope-ratio mass spectrometer (Finnigan MAT). The elemental analyzer combusted samples in
183 pure O_2 , resultant gasses were reduced to N_2 and CO_2 and passed through a series of thermal
184 conductivity detectors and element traps to determine percent compositions. Besides isotopes,
185 this method also provided bulk elemental composition (%) for carbon and nitrogen. Acetanilide
186 ($\text{C}_8\text{H}_9\text{NO}$: 71.09% C; 10.36 % N) was the calibrant. We sent a small subset of additional samples
187 ($n < 20$) to the Biogeochemical Stable Isotope Facility at the University of Hawaii, where similar
188 analyses and procedures were followed.

189 We expressed sample stable isotope ratios relative to the isotope standard following
190 conventional delta (δ) notation in parts per thousand (‰), using $\delta = ([R_{\text{sample}}/R_{\text{standard}}] - 1) \cdot (1000)$,
191 where R_{sample} and R_{standard} are the corresponding ratios of heavy to light isotopes (e.g., $^{15}\text{N}/^{14}\text{N}$) in
192 the sample and standard, respectively. R_{standard} for ^{13}C was Baker Acetanilide ($\delta^{13}\text{C} = -10.4$)
193 calibrated monthly against the Peedee Belemnite limestone formation international standard. The
194 R_{standard} for ^{15}N was IAEA N1 Ammonium Sulfate/ $(\text{NH}_4)_2\text{SO}_4$ ($\delta^{15}\text{N} = 0.4$) calibrated monthly
195 against atmospheric N_2 and USGS nitrogen standards. All analytical runs included known
196 standards placed every 6-7 samples to calibrate against instrument drift. Hundreds of replicate
197 assays of reference materials indicated measurement errors of 0.06‰ for carbon and 0.12‰ for N
198 for this setup (e.g., Seminoff et al. 2006; Seminoff et al. 2012).

199 We generated a series of visualizations from the scute imaging and SIA data, with a few
200 provisions. First, the Caribbean hawksbill scutes alone were disintegrated from the original
201 carapace with no accompanying demographic data. For these scutes, we previously (see Miller et
202 al. 2019) estimated the straight carapace length (“SCL”) of the turtle from which they originated
203 from the area of individual scutes. Second, in plotting the stable isotope values from scute
204 microsampling, we recognized that drilled transect paths always exceeded individual growth
205 lines, and at times imperfectly followed growth line contours (range = 2–35 growth lines, mean =
206 6.1). As a result, we recorded the minimum and maximum growth line number of each transect
207 drill path and plotted SIA results graphically against the median growth line.

208 Third, to compare isotope trajectories through development between samples, we
209 generated an ensemble model for $\delta^{13}\text{C}$ and $\delta^{15}\text{N}$ values across development. As we have no
210 telemetry or genetics data to indicate these adjoining regions hold completely distinct populations
211 (Gaos et al. 2020), we conservatively pooled data from all North Pacific turtles (Central and
212 Western Pacific). The resulting ensemble is a locally-weighted regression (Cleveland and Devlin
213 1988) of the average stable isotope values in each 10 growth line wide bin (lines 0–9, 10–19...
214 190–199, etc.) of the median microsampled position value. We use this not to make population
215 inferences, but only to illustrate a stage-specific stable isotope value reference. To augment
216 sample sizes in each of these bins (range: 1–7 samples, mean 3.1 samples), we added the results
217 from the previous ventral surface scrapings from the Hawaii samples only. For these samples, the
218 growth line number attributed to the sample was the maximum growth line number for that
219 individual. [Here, growth lines were calculated and described in a previous study (Van Houtan et
220 al. 2016a).] We excluded hatchling data as well as data originating from scutes from other ocean
221 subbasins from these ensemble models.

222 We previously aged turtles through a validated, bomb radiocarbon $\delta^{14}\text{C}$ method or
223 estimated age from a derived von Bertalanffy growth function (Van Houtan et al. 2016a). As the
224 PM for one individual turtle was worn (see below), its early tissue record is absent, and its
225 discernable count of growth lines ($n = 110$) is truncated. As a result, we estimated its total growth
226 line count ($n = 200$) from a derived length-to-growth-line model (Van Houtan et al. 2016a) and
227 plot its isotope data beginning at the difference between that estimate and its documented count
228 (e.g., 90).

229

230 RESULTS

231 Sampling the ventral surfaces of central scutes does not indicate a clear stable isotope pattern
232 throughout development, though it suggests some regional structure. Fig. 1 plots the $\delta^{13}\text{C}$ and
233 $\delta^{15}\text{N}$ values and bulk carbon and nitrogen content from scute surface samples from $n = 106$
234 hawksbills. Of these samples, 28 originated from Hawaii (4.0–88.7 SCL), 60 from Caribbean
235 (38.5–84.3 SCL), and 18 from American Samoa (27.7–68.4 SCL). Scatter and density plots show
236 somewhat clustered and normally distributed $\delta^{13}\text{C}$ values (Fig. 1AB, -15.8 ± 1.32 ‰, 95% CI: -

237 18.3 to -13.2 ‰), but simple linear regressions reveal no significant trends across development
238 ($F_{1,105} = 0.002$, $P = 0.97$, adjusted $R^2 = -0.01$). The $\delta^{15}\text{N}$ plots (Fig. 1 CD) indicate more spread in
239 the N isotope data (10.0 ± 2.48 ‰, 95% CI: 5.1–14.9 ‰). This is evidenced in the long tail
240 towards heavier N isotopes (Fig. 1D) and as 6 American Samoa juveniles and 2 Hawaii adults are
241 heavier than the 95% CI for $\delta^{15}\text{N}$ (Fig. 1C). Simple linear regression suggests significant $\delta^{15}\text{N}$
242 changes over development ($F_{1,105} = 4.73$, $P = 0.03$), however, the model's explanatory power is
243 weak (adjusted $R^2 = 0.03$). When regions were considered separately, the $\delta^{13}\text{C}$ (-16.1 ± 1.38 ‰)
244 and $\delta^{15}\text{N}$ (10.1 ± 2.29 ‰) values from Hawaii are consistent with the pooled results. The
245 American Samoa ($\delta^{13}\text{C}$: -16.9 ± 1.44 ‰; $\delta^{15}\text{N}$: 13.7 ± 2.85 ‰) and Caribbean ($\delta^{13}\text{C}$: -15.3 ± 0.95
246 ‰; $\delta^{15}\text{N}$: 8.8 ± 0.86 ‰) also overlap with the pooled results but show more $\delta^{15}\text{N}$ structure. Fig.
247 1EF details the bulk elemental composition, with carbon = $48.9 \pm 1.37\%$, N = $14.7 \pm 0.63\%$, and
248 the remaining 36.4% arising from H, O, S, and other elements. The C:N ratio for all ventral scute
249 surface samples was 3.33 ± 0.08 . Table S1 provides further details on sample metadata. As the
250 SCL domains differ between regional sample groups, we cannot rigorously model population
251 differences in stable isotopes. However, the stable isotope values from these surface samples
252 show no clear developmental trends.

253 Fig. 2 illustrates a general model that ultimate PM scutes capture growth continuously
254 throughout development, containing a near-complete life history record. Fig. 2A locates the left
255 ultimate PM scute on a dry-archived, juvenile hawksbill carapace, and the ventral surface regions
256 sampled (white dashed line rectangle). When sectioned sagittally and polished, these PM scutes
257 reveal internal incremental growth layers (Fig. 2B). Parallel growth layers occur on either side of
258 the central suture line, where the dorsal carapace and ventral plastron fuse. Here in this 44.2-cm
259 SCL juvenile, the PM contained 50 growth lines. Bomb radiocarbon techniques aged this turtle at
260 6.8 years, suggesting it deposited an average of 7 growth lines annually (Van Houtan et al.
261 2016a).

262 Continuous sampling of $\delta^{13}\text{C}$ and $\delta^{15}\text{N}$ values throughout the life history of 6 Hawaii
263 hawksbill turtles, reveals individual life histories, but no consistent pattern (Fig. 3). Only 1 turtle
264 shows a clear ontogenetic shift indicated by abrupt coincident changes in the $\delta^{13}\text{C}$ and $\delta^{15}\text{N}$
265 values between the early and late growth lines sampled (Fig. 3F). Here, $\delta^{13}\text{C}$ values decrease from
266 growth lines 0–60 and then flatten out near -16 ‰ $\delta^{13}\text{C}$. By contrast, $\delta^{15}\text{N}$ values increase through
267 development, jumping from near 6 ‰ to near 15 ‰ $\delta^{15}\text{N}$ between growth lines 40 to 60. When
268 the full isoscape for this turtle is plotted ($\delta^{15}\text{N}$ plotted against $\delta^{13}\text{C}$) a dramatic dietary (and/or
269 habitat) shift is apparent (highlighted by the orange arrow, Fig. 3F). This pattern suggests a
270 discrete biogeographical and developmental phase shift, perhaps being an early life history shift
271 from pelagic to neritic ecosystems (Reich et al. 2007; Bjorndal and Bolten 2010). The remaining
272 5 turtles reveal more subtle patterns and suggest no distinct developmental biogeography. Fig. 3A
273 and 3E show a slight decrease of $\delta^{13}\text{C}$ values in growth lines 0–40, but the accompanying $\delta^{15}\text{N}$
274 values are either absent or constant. Two turtles (Fig. 3BC) show a gradual enrichment in $\delta^{13}\text{C}$ in
275 growth lines 0–80 but reveal no significant $\delta^{15}\text{N}$ patterns. The last turtle (Fig. 3D) abraded its
276 early life history tissue, so this record is lost, but has remarkably constant $\delta^{13}\text{C}$ and $\delta^{15}\text{N}$ values
277 throughout. Fig. 3G shows the geographic origins of the samples in the Main Hawaiian Islands,
278 unless unknown (Fig. 3E). Though the ^{13}C Suess effect is seemingly strongest in the surface
279 waters of the North Pacific (Eide et al. 2017) it seems an unlikely influence to these patterns as
280 we observe no consistent $\delta^{13}\text{C}$ trend, and its magnitude is weak (< 0.02 ‰ yr^{-1}) to our observed
281 changes (Figure 3).

282 Continuous PM microsampling of stable isotope values for 3 Western Pacific hawksbills
283 suggests ontogenetic shifts across isotopically distinct areas might be more common in this region
284 (Fig. 4). Despite a lack of adult tissues (these juveniles measured 42–50 cm SCL, estimated at 5–7
285 years old) each turtle shows some evidence of a distinct developmental shift. Here, individual

286 isoscape plots of $\delta^{13}\text{C}$ against $\delta^{15}\text{N}$ are particularly revealing with each showing two clusters of
287 data points. Though these isotope data suggest developmental changes to diet and ecosystem
288 through development, they do not record the same pattern across turtles. The isoscape clusters
289 reveal dramatic $\delta^{13}\text{C}$ increases with gradual $\delta^{15}\text{N}$ increases (Fig. 4A), gradual $\delta^{13}\text{C}$ declines with
290 dramatic $\delta^{15}\text{N}$ declines (Fig. 4B), and significant $\delta^{13}\text{C}$ increases with significant $\delta^{15}\text{N}$ declines
291 (Fig. 4C). Like the Hawaii hawksbills in Fig. 3, there is no clear agreement in overall pattern. Fig.
292 4D shows the geographic origin of these turtles in Palau and the Marshall Islands, and origin of
293 some of the forage samples in Fig. 5.

294 Though non-exhaustive, Fig. 5 summarizes available bulk stable isotope values of typical
295 hawksbill forage items from 4 Pacific Ocean regions. The data comprise 89 samples from 36
296 morphospecies representing 5 major forage groups: sponges, other macroinvertebrates, red algae,
297 green algae, and brown algae. Hawksbills are omnivores and while this dataset is not exhaustive,
298 it represents all known forage groups for hawksbills in this region (Graham 2009). Based on the
299 limited data from these samples, the isoscape reveals some apparent structure of hawksbill forage
300 items between Pacific regions. This is particularly true for $\delta^{15}\text{N}$ values. The macroinvertebrates
301 and sponges of Palmyra Atoll ($\delta^{15}\text{N} > 9\text{‰}$), for example, have $\delta^{15}\text{N}$ values almost twice that of
302 the same groups in the Main Hawaiian Islands ($\delta^{15}\text{N} < 5\text{‰}$). The macroinvertebrates and sponges
303 sampled from Kwajalein Atoll are between the two extremes with $\delta^{15}\text{N}$ values near 7‰. Across
304 locations and forage groups, $\delta^{13}\text{C}$ values are highly variable by comparison with $\delta^{15}\text{N}$ values. The
305 limited representation of only green algae from Rose Atoll shows high variability in both $\delta^{13}\text{C}$
306 and $\delta^{15}\text{N}$ values. Tables S2 provides more details on these forage items, including species and
307 samples sizes.

308

309 DISCUSSION

310 Given their critical conservation status and ongoing exploitation (Mortimer and Donnelly 2008;
311 Miller et al. 2019), understanding the spatial population structure of hawksbill sea turtles may be
312 important for developing effective management strategies (Monzón-Argüello et al. 2010; Wallace
313 et al. 2010; Seminoff et al. 2015). This may require a dedicated endeavor for hawksbills,
314 however, as their omnivorous and variable life history traits defy simple characterization,
315 especially among disparate regional populations. Unlike other sea turtle species, satellite
316 telemetry (Hawkes et al. 2012; Marcovaldi et al. 2012; Walcott et al. 2012) and fishery bycatch
317 data (Van Houtan et al. 2016b) reveal no clear developmental biogeography for hawksbills.
318 Furthermore, intensive habitat use studies indicate that much remains cryptic about hawksbill life
319 history (Gaos et al. 2012; Liles et al. 2015). Together, this may suggest for hawksbills that at
320 regional and global scales the pattern may be that there is no typical pattern.

321 Diagnostic tissue analysis may help supplement other data streams and be useful to
322 resolve life history questions. Early, limited analysis of homogenized outer scute layers from 2
323 Florida and 2 Bahamas hawksbills had mean $\delta^{15}\text{N}$ of $\sim 5.5\text{‰}$ and $\delta^{13}\text{C}$ of $\sim -17\text{‰}$ (Reich et al.
324 2007), providing the first insights into hawksbill scute stable isotopes. Comparing distinct
325 developmental stages of scute growth layers in nesting females from the Lesser Antilles, Fireman
326 (2021) found highly variable stable isotope values (mean: $\delta^{15}\text{N} = 8.9\text{‰}$, $\delta^{13}\text{C} = -13.4\text{‰}$) and
327 clear evidence of ontogenetic shifts in just 8% (4 of 50) of sampled individuals. Whole blood and
328 skin biopsy analysis from juvenile hawksbills in the eastern tropical Pacific of Costa Rica show a
329 broad $\delta^{13}\text{C}$ niche (range: -19 to -13‰) by comparison to $\delta^{15}\text{N}$ (range: 12 to $\sim 14\text{‰}$) (Clyde-
330 Brockway et al. 2022). Biopsy samples of 4 scute growth layers in juvenile and subadult
331 hawksbills in the eastern tropical Pacific of Nicaragua and El Salvador showed a general
332 depletion through growth across a broad range of $\delta^{13}\text{C}$ values (range: -27 to -17‰) (Wedemeyer-
333 Strombel et al. 2021). Longitudinal skeletal sampling of hawksbills in the eastern tropical Pacific

334 of El Salvador shows consistent decline through development of $\delta^{13}\text{C}$ (from ~ -15 to ~ -24) and
335 $\delta^{15}\text{N}$ (from ~ 14 to ~ 11), indicating an oceanic to nearshore shift (Turner Tomaszewicz et al.
336 2022).

337 Here we provide a novel longitudinal record of stable isotopes in the keratin growth
338 layers of carapace PM scutes for underrepresented populations. Our overarching result is the
339 documentation of multiple types of development and habitat use. The initial ventral surface
340 sampling shows no clear patterns of isotope depletion or enrichment across development from
341 hatchlings to breeding females (Fig. 1), but like skin or blood samples, this technique summarizes
342 a life history record that is both recent and brief. Analogous to tree rings (Schweingruber 2012)
343 and fish otoliths (Pannella 1971), cross-sectioned and polished PM scutes reveal a near-complete
344 tissue record (Fig. 2) with potential to yield new insights into age, diet, and migrations (Van
345 Houtan et al. 2016a). For Hawaiian hawksbills, only 1 of 6 turtles (17%) has clear evidence of an
346 ontogenetic shift (Fig. 3). This corroborates a previous analysis of bycatch, strandings, and
347 opportunistic observations that hawksbills aged 0–4 years mostly remain in the coastal waters of
348 Hawaii (Van Houtan et al. 2016b). This proportion, however, is roughly consistent with what has
349 been inferred from isotopes from hawksbills from the Lesser Antilles (Fireman 2021), but is
350 significantly less than the eastern tropical Pacific populations (Wedemeyer-Strombel et al. 2021;
351 Turner Tomaszewicz et al. 2022). The longitudinal stable carbon records of Hawaii hawksbills
352 further disagree, containing both patterns of ^{13}C enrichment and depletion through development
353 (Fig. 3). By contrast to the Hawaii specimens, all 3 Western Pacific turtles show a clear
354 ontogenetic shift. However, the isoscape plots reveal perhaps 3 different types of shifts and no
355 single habitat-use pattern (see orange arrows in Fig. 4A–C). Together this suggests that the early
356 development phase of Western Pacific hawksbills may have less association with nearshore
357 waters, specifically by comparison to Hawaii hawksbills. While such sequential and repeated
358 sampling within individual tissues holds promise, especially as a complement to other sampling
359 techniques, the present analysis represents a small sample and should be expanded.

360 Beyond providing new information about individual migrations, our results add to a
361 growing body of evidence that tissue isotopes vary regionally between hawksbill populations.
362 Fig. 1 shows a gradual structure in scute N isotopes between Caribbean, Central Pacific, and
363 South Pacific populations that is consistent with the isotopes of regional forage items (Fig. 5),
364 Caribbean hawksbill scutes (Reich et al. 2007; Fireman 2021), and other reef taxa in these regions
365 (Cocheretdelamorinière et al. 2003; Fiore et al. 2013). Across hawksbill populations, there
366 remains a substantial need to document the site-specific dietary composition and forage
367 characteristics, however. While recent studies are encouraging (Méndez-Salgado et al. 2020;
368 Clyde-Brockway et al. 2022; Turner Tomaszewicz et al. 2022), most geographic regions are
369 persistently data poor, limiting ecological knowledge and conservation planning for the species.
370 Future studies should therefore expand ecological monitoring efforts to increase data collection
371 on the habitat use and foraging ecology of hawksbills as well as the diagnostic analysis of their
372 forage items. Of note, the regional $\delta^{15}\text{N}$ patterns we describe here (Fig. 1C–D) from hawksbill
373 scutes parallel the differences in seabird trophic position from the same marine regions (see Fig.
374 S1) which have been correlated with anthropogenic factors (Gagné et al. 2018a). As $\delta^{15}\text{N}$ patterns
375 of consumers are derived from ^{15}N values at the food web base, future work may investigate
376 whether these values are fixed in time or whether they are impacted by anthropogenic pressures
377 such as overfishing and climatic change.

378 Fig. 5 summarizes available stable isotope values for common hawksbill forage items in
379 the Central, South, and Western Pacific. As these forage data are not exhaustive, we are
380 prevented from running a formal mixing model (Lemons et al. 2011; Stock and Semmens 2016;
381 Gagné et al. 2018b; Stock et al. 2018), and cannot infer diets or dietary shifts through
382 development for these individuals. From the data we possess, however, one thing may be clear.

383 The sampled forage items from Hawaii are relatively exhaustive (41 samples from 21 species
384 across 5 forage groups, see Table S2), have $\delta^{15}\text{N}$ values ranging from 2–5 ‰, yet are somehow
385 lacking the full complement of hawksbill prey species. While the mean $\delta^{15}\text{N}$ values across
386 development for Hawaii hawksbills in Fig. 3 is ≥ 9 ‰, two adult turtles (Fig. 3C, F) have $\delta^{15}\text{N}$
387 values that exceed 15 ‰. Given that published sea turtle tissue $\delta^{15}\text{N}$ discrimination values are \leq
388 4.0 ‰ (Seminoff et al. 2006; Vander Zanden et al. 2012), these 2 adults are likely consuming
389 items not displayed in Fig. 5. A possible explanation is that these individuals recently migrated
390 from another region with heavier N forage. However, this is unlikely given the isolation of the
391 Hawaiian archipelago, and that none of the foraging items for any Pacific regions in Fig. 5 can
392 support such high tissue $\delta^{15}\text{N}$ values. Since these turtles both stranded in the 1980s, these turtles
393 may have foraged on high-trophic level species that no longer occur in such abundance, or this
394 may be reflecting that food web compression has occurred in recent decades in Hawaii's reef
395 ecosystems. Another explanation is that these individuals foraged in impaired watersheds with
396 high N footprints (e.g., Van Houtan et al. 2010). However, such influences are thought to be
397 greater in subsequent decades yet are not observed in hawksbills from these later time periods.

398 Resolving individual life histories through the longitudinal analysis of hawksbill scutes
399 shows promise, but much work remains. In this study we expand on earlier pioneering studies
400 that first demonstrated successional layering in hawksbill scutes (Tucker et al. 2001; Palaniappan
401 2007), and later documented a near-complete chronology in the ultimate PM scutes (Van Houtan
402 et al. 2016a). Using the same tissues and preparations, here we sequentially sampled along scute
403 growth line contours and performed SIA to understand individual life histories and regional
404 population structure. As we have shown, especially when combined with other traditional and
405 diagnostic tools, such methods can reveal previously unknown information with obvious
406 conservation applications.

407 Moving forward, future progress can be made in several distinct ways. The novel
408 sclerochronology methods we developed here can be applied universally to reconstruct the long-
409 term habitat use of individual hawksbill sea turtles in any geographic region. We recommend
410 expanding the approach to increase both the samples and populations analyzed here. This might
411 prioritize data poor regions of the South Atlantic, Indian, West Pacific and South Pacific basins as
412 well as the Eastern Pacific and the Northwest Atlantic. We also recommend refining our
413 techniques with ultimate PM scutes, comparing it with other scute tissues, and further aligning it
414 with growth line and ageing studies (e.g. Van Houtan et al. 2016a). As it was here, partnerships
415 with museums, natural history repositories, law enforcement agencies, and stranding programs
416 may be important to obtain specimens as well as to demonstrate additional applied contexts for
417 such isotopic research (Espinoza et al. 2007). In addition to replicating and refining this work, we
418 recommend supplementing the existing mass spectrometry diagnostics of carbon and nitrogen to
419 additional elements. As Fig. 1E-F demonstrates, 36% of scute tissues are composed of H, O, S,
420 and other trace elements. Although H and O can display low variability between regions, δD ,
421 $\delta^{18}\text{O}$, and $\delta^{34}\text{S}$ have demonstrated use in marine systems (Cardona et al. 2009; Clark and Fritz
422 2013; Tucker et al. 2014; Duarte et al. 2018; Miller et al. 2019) and may be useful for sea turtle
423 populations. Together, these programs will allow for the development of robust mixing models,
424 advance our understanding of individual life histories, and increase the effectiveness of
425 conservation management for critically endangered hawksbill sea turtles.

426

427 **ACKNOWLEDGEMENTS:** R. Humphreys provided access to laboratory space and equipment;
428 J. Sampaga, E. Di Martini, A. Andrews, and B. Taylor advised on life history analysis methods.
429 S. Murakawa, S. Brunson, D. Francke, A. Niccum, N. Sarto, and R. Dollar assisted with
430 necropsies and specimen preparations. G. Balazs, G. Phocas, A. Palermo, C. King, and W. Seitz
431 provided specimens; B. Tibbats and C. Smith assisted with forage samples. A. Copenhaver and L.

432 Kaneshiro provided program support. C. Turner Tomaszewicz and 2 anonymous reviewers
433 provided helpful comments on earlier versions of this manuscript.

434 **AUTHOR CONTRIBUTIONS:** KV and JAS designed the study and wrote the manuscript. KV,
435 TJ, MH, and GP provided and prepared specimens. JAS and JS performed the diagnostic
436 analyses, while KV analyzed the data and generated the figures. All authors made contributions to
437 and reviewed the manuscript.

438 **ETHICS STATEMENT:** All research followed the NOAA Institutional Animal Care and Use
439 Committee criteria.

440 **DATA ACCESSIBILITY:** Raw data and high-resolution figures are available at an independent
441 third-party repository at the Open Science Framework <https://osf.io/2fh39/>.

442 **COMPETING INTERESTS:** The authors declare no competing interests

443

444 **FIGURE CAPTIONS**

445 **Figure 1. Bulk stable isotope and elemental composition from the ventral surfaces of**
446 **hawksbill carapace scutes.** (A) Raw results and (B) density of $\delta^{13}\text{C}$ content ($-15.8 \pm 1.32 \text{ ‰}$),
447 with (C) raw results and (D) density of $\delta^{15}\text{N}$ values ($10.0 \pm 2.48 \text{ ‰}$). Filled shapes are individual
448 turtles comprising 10 hatchlings (4–5 cm SCL), 77 juveniles (28–71 cm SCL), and 19 adults (72–
449 89 cm SCL) from Hawaii (grey circles), Caribbean (purple squares), and American Samoa
450 (orange triangles) populations. Horizontal grey lines are the normalized 95% interval of all 106
451 samples. Simple linear regressions of both series (adjusted correlation coefficients listed) show no
452 trend through development. Density plots of (E) carbon and (F) nitrogen composition (expressed
453 as a percentage, median values listed) indicate 36.4% of scute material is exclusive of carbon and
454 nitrogen. Sampled tissue is from the ventral scute surfaces and captures the ecosystem experience
455 preceding each turtle's demise. Hatchlings are ecologically naïve, and their tissues are maternally
456 derived. As we lack samples from 8–28 cm SCL (0–4 years old) these plots do not represent the
457 cryptic early life history phase.

458 **Figure 2. Unlike surface material, cross sections of posterior marginal (PM) scutes from**
459 **hawksbills contain a longitudinal chronology.** (A) Dorsal carapace view of a 44.2 cm SCL
460 juvenile Hawaii hawksbill with the left ultimate PM removed. PM scutes both retain the largest
461 keratin archives on the shell and can be less frequently damaged than carapace scutes. White
462 dashed rectangle indicates the ventral surface region sampled in Figure 1. (B) PM sagittal cross
463 section reveals a chronology of growth lines, with tissue accretion from left (posterior, old) to
464 right (anterior, new). Cross section polished to 1 mm thickness and imaged under magnification
465 using a combination of reflected and transmitted light. This turtle had 50 growth lines, with every
466 tenth contour labelled and highlighted for clarity.

467 **Figure 3. Stable isotope values from scute growth contours shows several developmental**
468 **patterns in Hawaii hawksbills.** (A–F) Imaged cross sections, drilled transects, and stable isotope
469 results for 6 hawksbill turtles. Hollow circle $\delta^{13}\text{C}$ values and age estimates are from a previous
470 study (Van Houtan et al. 2016a), filled circles are from the current study. Black lines interpolate
471 values, are a LOESS when multiple data sources are available, and grey line is the ensemble
472 average for all individuals (Figs. 3–4). From left to right (A–D, F) or top to bottom (D), drill line
473 paths increase in age. Juvenile tissue in one turtle (D) is missing from abrasion. (G) Map of the
474 Hawaiian archipelago locates each turtle's stranding site (E is unknown). There is no single
475 pattern in either carbon or nitrogen isotopes across development envisioned in either single or
476 dual variable plots. (F) Apparently demonstrates a discrete habitat shift (orange arrow), reflected
477 in $\delta^{13}\text{C}$ and $\delta^{15}\text{N}$ values, perhaps due to nearshore settlement. Gradual shifts in $\delta^{13}\text{C}$ values (A–B,

478 E) and (E) also indicate potential habitat shifts. Scale bar is 5 mm. Asterisk (*) indicates turtle
479 age estimated with a Von Bertalanffy growth function (see Methods).

480 **Figure 4. Stable isotope values from scute growth contours of Western Pacific hawksbills.**
481 Though the turtles from (A) Palau and (B-C) Kwajalein Atoll are all relatively young, stable
482 isotopes document potential shifts in both habitat and forage. Symbology retained from Figure 3,
483 scale bars are 5 mm. Asterisk (*) indicates age estimated using measured length and previously
484 derived VBGF parameters (Van Houtan et al. 2016a) as we had no date metadata for this
485 specimen. Stranding dates of (B-C) allow us to estimate birth year; (A) has no stranding date.
486 Orange arrows indicate an apparent habitat and dietary shift. (D) Map of the central and Western
487 Pacific with all sample collection regions noted.

488 **Figure 5. Stable isotope values of typical hawksbill forage item groups from four Pacific**
489 **Island regions.** Hawksbills are omnivores that forage on sponges, other macroinvertebrates, and
490 macroalgae. Above stable isotope values are crowdsourced from the literature (Palmyra Atoll,
491 Pacific Remote Island Areas USA), our own collection efforts (Kwajalein Atoll, Marshall Islands;
492 Rose Atoll, American Samoa), or a combination of both (Main Hawaiian Islands). Filled circles
493 represent the group mean, lines are standard error. Though there is significant variability in $\delta^{13}\text{C}$
494 values within each region, and sometimes within a single region's forage item groups, there is
495 some structure of $\delta^{15}\text{N}$ values between regions. These data are meant to report what currently
496 exists, but not represent an exhaustive list of all potential hawksbill forage items in all population
497 regions.

498
499

500 CITATIONS

- 501 Avens L, Goshe LR, Pajuelo M, Bjorndal KA, MacDonald BD, Lemons GE, Bolten AB, Seminoff JA (2013) Complementary
502 skeletochronology and stable isotope analyses offer new insight into juvenile loggerhead sea turtle oceanic stage duration and
503 growth dynamics. *Mar Ecol Progr Ser* 491: 235-251
- 504 Avens L, Ramirez MD, Hall AG, Snover ML, Haas HL, Godfrey MH, Goshe LR, Cook M, Heppell SS (2020) Regional differences in
505 Kemp's ridley sea turtle growth trajectories and expected age at maturation. *Marine Ecology Progress Series* 654: 143-161
- 506 Balazs GH, Van Houtan KS, Hargrove SA, Brunson SM, Murakawa SK (2015) A review of the demographic features of Hawaiian
507 green turtles (*Chelonia mydas*). *Chelonian Conserv Biol* 14: 119-129
- 508 Becker B, Kromer B, Trumbore P (1991) A stable-isotope tree-ring timescale of the Late Glacial/Holocene boundary. *Nature* 353:
509 647-649
- 510 Bjorndal KA, Bolten AB (2010) Hawksbill sea turtles in seagrass pastures: success in a peripheral habitat. *Marine Biology* 157: 135-
511 145 doi 10.1007/s00227-009-1304-0
- 512 Brunson S, Gaos AR, Kelly IK, Van Houtan KS, Swimmer Y, Hargrove S, Balazs GH, Work TM, Jones TT (2022) Three decades of
513 stranding data reveal insights into endangered hawksbill sea turtles in Hawai'i. *Endang Spec Res* 47: 109-118
- 514 Caine EA (1986) Carapace epibionts of nesting loggerhead sea turtles: Atlantic coast of USA. *J Exper Mar Biol Ecol* 95: 15-26
- 515 Cardona L, Aguilar A, Pazos L (2009) Delayed ontogenetic dietary shift and high levels of omnivory in green turtles (*Chelonia mydas*)
516 from the NW coast of Africa. *Mar Biol* 156: 1487-1495 doi 10.1007/s00227-009-1188-z
- 517 Clark ID, Fritz P (2013) *Environmental isotopes in hydrogeology*. CRC press
- 518 Cleveland WS, Devlin SJ (1988) Locally Weighted Regression: An Approach to Regression Analysis by Local Fitting. *J Am Stat*
519 *Assoc* 83: 596-610
- 520 Clyde-Brockway CE, Heidemeyer M, Paladino FV, Flaherty EA (2022) Diet and foraging niche flexibility in green and hawksbill
521 turtles. *Marine Biology* 169: 108 doi 10.1007/s00227-022-04092-1
- 522 CocheretdelaMorinière EC, Pollux B, Nagelkerken I, Hemminga M, Huiskes A, van der Velde G (2003) Ontogenetic dietary changes
523 of coral reef fishes in the mangrove-seagrass-reef continuum: stable isotopes and gut-content analysis. *Marine Ecology Progress*
524 *Series* 246: 279-289
- 525 Dailer ML, Knox RS, Smith JE, Napier M, Smith CM (2010) Using $\delta^{15}\text{N}$ values in algal tissue to map locations and potential sources
526 of anthropogenic nutrient inputs on the island of Maui, Hawaii, USA. *Mar Poll Bull* 60: 655-671
- 527 Deniro MJ, Epstein S (1981) Influence of diet on the distribution of nitrogen isotopes in animals. *Geochimica et Cosmochimica Acta*
528 45: 341-351 doi [http://dx.doi.org/10.1016/0016-7037\(81\)90244-1](http://dx.doi.org/10.1016/0016-7037(81)90244-1)
- 529 Donnelly M (2008) Trade routes for tortoiseshell. SWOT Report III: 24-25
- 530 Duarte CM, Delgado-Huertas A, Anton A, Carrillo-de-Albornoz P, López-Sandoval DC, Agustí S, Almahasheer H, Marbá N,
531 Hendriks IE, Krause-Jensen D, Garcias-Bonet N (2018) Stable Isotope ($\delta^{13}\text{C}$, $\delta^{15}\text{N}$, $\delta^{18}\text{O}$, δD) Composition and Nutrient
532 Concentration of Red Sea Primary Producers. *Front Mari Sci* 5 doi 10.3389/fmars.2018.00298
- 533 Eide M, Olsen A, Ninnemann US, Eldevik T (2017) A global estimate of the full oceanic ^{13}C Suess effect since the preindustrial.
534 *Global Biogeochemical Cycles* 31: 492-514
- 535 Espinoza EO, Baker BW, Berry CA (2007) The analysis of sea turtle EO and bovid keratin artefacts using drift spectroscopy and
536 discriminant analysis. *Archaeometry* 49: 685-698

537 Fiore CL, Baker DM, Lesser MP (2013) Nitrogen Biogeochemistry in the Caribbean Sponge, *Xestospongia muta*: A Source or Sink of
538 Dissolved Inorganic Nitrogen? PLOS ONE 8: e72961 doi 10.1371/journal.pone.0072961

539 Fireman AL (2021) On the Shell of the Turtle: Identifying the Isotopic Niche of Hawksbill Sea Turtles in Antigua, West Indies
540 Gagné TO, Hyrenbach KD, Hagemann ME, Bass OL, Pimm SL, MacDonald M, Peck B, Houtan KSV (2018a) Seabird trophic
541 position across three ocean regions tracks ecosystem differences. Front Mari Sci 5: 317

542 Gagné TO, Hyrenbach KD, Hagemann ME, Van Houtan KS (2018b) Trophic signatures of seabirds suggest shifts in oceanic
543 ecosystems. Science advances 4: eaao3946

544 Gaos AR, Kurpita L, Bernard H, Sundquist L, King CS, Browning JH, Naboa E, Kelly IK, Downs K, Eguchi T (2021) Hawksbill
545 nesting in Hawai'i: 30-year dataset reveals recent positive trend for a small, yet vital population. Front Mari Sci: 1719

546 Gaos AR, LaCasella EL, Kurpita L, Balazs G, Hargrove S, King C, Bernard H, Jones TT, Dutton PH (2020) Hawaiian hawksbills: a
547 distinct and isolated nesting colony in the Central North Pacific Ocean revealed by mitochondrial DNA. Conservation Genetics
548 21: 771-783

549 Gaos AR, Lewison RL, Yañez IL, Wallace BP, Liles MJ, Nichols WJ, Baquero A, Hasbún CR, Vasquez M, Urteaga J (2012) Shifting
550 the life-history paradigm: discovery of novel habitat use by hawksbill turtles. Biol Lett 8: 54-56

551 Graham SC (2009) Analysis of the foraging ecology of hawksbill turtles (*Eretmochelys imbricata*) on Hawai'i Island: An investigation
552 utilizing satellite tracking and stable isotopes. University of Hawaii (Hilo, HI), MSc thesis

553 Grottoli AG, Eakin CM (2007) A review of modern coral $\delta^{18}\text{O}$ and $\Delta^{14}\text{C}$ proxy records. Earth-Science Rev 81: 67-91

554 Hawkes L, Tomás J, Revuelta O, León Y, Blumenthal J, Broderick A, Fish M, Raga J, Witt M, Godley B (2012) Migratory patterns in
555 hawksbill turtles described by satellite tracking. Mar Ecol Progr Ser 461: 223-232

556 Hobson KA, Wassenaar LI (2008) Tracking animal migration with stable isotopes. Academic Press

557 Kelly EB (2012) Using Stable Isotope Analysis to Assess the Foraging Habits of Palmyra Atoll Green Turtles (*Chelonia mydas*).
558 Columbia University (New York, NY), MSc thesis

559 Lemons G, Lewison R, Komoroske L, Gaos A, Lai C-T, Dutton P, Eguchi T, LeRoux R, Seminoff JA (2011) Trophic ecology of
560 green sea turtles in a highly urbanized bay: insights from stable isotopes and mixing models. J Exper Mar Biol Ecol 405: 25-32

561 Liles MJ, Peterson MJ, Seminoff JA, Altamirano E, Henríquez AV, Gaos AR, Gadea V, Urteaga J, Torres P, Wallace BP (2015) One
562 size does not fit all: importance of adjusting conservation practices for endangered hawksbill turtles to address local nesting
563 habitat needs in the eastern Pacific Ocean. Biol Conserv 184: 405-413

564 Marcovaldi MÂ, Lopez GG, Soares LS, López-Mendilaharsu M (2012) Satellite tracking of hawksbill turtles *Eretmochelys imbricata*
565 nesting in northern Bahia, Brazil: turtle movements and foraging destinations. Endang Spec Res 17: 123-132

566 Méndez-Salgado E, Chacón-Chaverri D, Fonseca LG, Seminoff JA (2020) Trophic ecology of hawksbill turtles (*Eretmochelys*
567 *imbricata*) in Golfo Dulce, Costa Rica: integrating esophageal lavage and stable isotope ($\delta^{13}\text{C}$, $\delta^{15}\text{N}$) analysis. Lat Am J Aquat
568 Res 48: 114-130

569 Miller EA, Lisin SE, Smith CM, Van Houtan KS (2020) Herbaria macroalgae as a proxy for historical upwelling trends in Central
570 California. Proc R Soc B 287: 20200732

571 Miller EA, McClenachan L, Uni Y, Phocas G, Hagemann ME, Van Houtan KS (2019) The historical development of complex global
572 trafficking networks for marine wildlife. Sci Advances 5: eaav5948

573 Monzón-Argüello C, Rico C, Naro-Maciél E, Varo-Cruz N, López P, Marco A, López-Jurado LF (2010) Population structure and
574 conservation implications for the loggerhead sea turtle of the Cape Verde Islands. Conserv Genet 11: 1871-1884

575 Mortimer JA, Donnelly M (2008) *Eretmochelys imbricata*. IUCN Red List of Threatened Species 2011.1: www.iucnredlist.org

576 Palaniappan PM (2007) The carapacial scutes of hawksbill turtles (*Eretmochelys imbricata*): development, growth dynamics and
577 utility as an age indicator. Charles Darwin University (Casuarina, NT, Australia), MSc thesis

578 Pannella G (1971) Fish otoliths: daily growth layers and periodical patterns. Science 173: 1124-1127

579 Popp B, Graham B, Olson R, Hannides C, Lott M, López-Ibarra G, Galván-Magaña F, Fry B (2007) Stable isotopes as indicators of
580 ecological change. New York: Academic Press

581 Ramirez MD, Avens L, Seminoff JA, Goshe LR, Heppell SS (2015) Patterns of loggerhead turtle ontogenetic shifts revealed through
582 isotopic analysis of annual skeletal growth increments. Ecosphere 6: 1-17 doi 10.1890/ES15-00255.1

583 Reich KJ, Bjorndal KA, Bolten AB (2007) The 'lost years' of green turtles: using stable isotopes to study cryptic lifestages. Biol Lett
584 3: 712-714

585 Schweingruber FH (2012) Tree rings: basics and applications of dendrochronology. Springer Science & Business Media

586 Seitz WA, Kagimoto KM, Luehrs B, Katahira L (2012) Twenty years of conservation and research findings of the Hawai'i Island
587 Hawksbill Turtle Recovery Project, 1989 to 2009. Pacific Cooperative Studies Unit Technical Report, University of Hawaii-
588 Manoa, Department of Botany, Honolulu, HI

589 Seminoff JA, Allen CD, Balazs GH, Dutton PH, Eguchi T, Haas H, Hargrove SA, Jensen M, Klemm DL, Lauritsen AM, Mac Pherson
590 SL, Opay P, Possardt EE, Pultz S, Van Houtan KS, Waples RS (2015) Status review of the green turtle (*Chelonia mydas*) under
591 the Engangered Species Act. NOAA Tech Memo NOAA-TM-NMFS-SWFSC-539: 599

592 Seminoff JA, Benson SR, Arthur KE, Eguchi T, Dutton PH, Tapilatu RF, Popp BN (2012) Stable isotope tracking of endangered sea
593 turtles: validation with satellite telemetry and $\delta^{15}\text{N}$ analysis of amino acids. PLoS ONE 7: e37403

594 Seminoff JA, Jones TT, Eguchi T, Jones DR, Dutton PH (2006) Stable isotope discrimination ($\delta^{13}\text{C}$ and $\delta^{15}\text{N}$) between soft tissues of
595 the green sea turtle *Chelonia mydas* and its diet. Mar Ecol Progr Ser 308: 271-278

596 Snover ML (2002) Growth and ontogeny of sea turtles using skeletochronology: methods, validation and application to conservation.
597 M.Sc. thesis: Duke University, Dureham, NC

598 Stock BC, Jackson AL, Ward EJ, Parnell AC, Phillips DL, Semmens BX (2018) Analyzing mixing systems using a new generation of
599 Bayesian tracer mixing models. PeerJ 6: e5096

600 Stock BC, Semmens BX (2016) Unifying error structures in commonly used biotracer mixing models. Ecology 97: 2562-2569

601 Trueman CN, MacKenzie K, Palmer M (2012) Identifying migrations in marine fishes through stable - isotope analysis. J Fish Biol
602 81: 826-847

603 Tucker AD, Broderick D, Kampe L (2001) Age estimation of *Eretmochelys imbricata* by sclerochronology of carapacial scutes.
604 Chelonian Conserv Biol 4: 219-222

605 Tucker AD, MacDonald BD, Seminoff JA (2014) Foraging site fidelity and stable isotope values of loggerhead turtles tracked in the
606 Gulf of Mexico and northwest Caribbean. Marine Ecology Progress Series 502: 267-279

607 Turner Tomaszewicz C, Liles M, Avens L, Seminoff J (2022) Tracking movements and growth of post-hatchling to adult hawksbill
608 sea turtles using skeleto+iso. *Front Ecol Evol* 10: 983260

609 Turner Tomaszewicz CN, Seminoff JA, Peckham SH, Avens L, Kurle CM (2017) Intrapopulation variability in the timing of
610 ontogenetic habitat shifts in sea turtles revealed using $\delta^{15}\text{N}$ values from bone growth rings. *J Anim Ecol* 86: 694-704 doi
611 10.1111/1365-2656.12618

612 Turner Tomaszewicz CN, Seminoff JA, Ramirez MD, Kurle CM (2015) Effects of demineralization on the stable isotope analysis of
613 bone samples. *Rapid Commun Mass Spectrom* 29: 1879-1888

614 Van Houtan KS, Andrews AH, Jones TT, Murakawa SKK, Hagemann ME (2016a) Time in tortoiseshell: a radiocarbon-validated
615 chronology in sea turtle scutes. *Proc R Soc B* 283

616 Van Houtan KS, Francke D, Alessi S, Jones TT, Martin SL, Kurpita L, King C (2016b) The developmental biogeography of hawksbill
617 sea turtles. *Ecol Evol* 6: 2378-2389

618 Van Houtan KS, Hargrove SK, Balazs GH (2010) Land use, macroalgae, and a tumor-forming disease in marine turtles. *PLoS One* 5:
619 e12900

620 Van Houtan KS, Hargrove SK, Balazs GH (2014a) Modeling sea turtle maturity age from partial life history records. *Pacific Science*
621 68: 465-477

622 Van Houtan KS, Smith CM, Dailer ML, Kawachi M (2014b) Eutrophication and the dietary promotion of sea turtle tumors. *PeerJ* 2:
623 e602 doi 10.7717/peerj.602

624 Vander Zanden HB, Bjorndal KA, Bolten AB (2013) Temporal consistency and individual specialization in resource use by green
625 turtles in successive life stages. *Oecologia* 173: 767-777 doi 10.1007/s00442-013-2655-2

626 Vander Zanden HB, Bjorndal KA, Mustin W, Ponciano JM, Bolten AB (2012) Inherent variation in stable isotope values and
627 discrimination factors in two life stages of green turtles. *Physiol Biochem Zool* 85: 431-441

628 Walcott J, Eckert S, Horrocks J (2012) Tracking hawksbill sea turtles (*Eretmochelys imbricata*) during inter-nesting intervals around
629 Barbados. *Marine Biology* 159: 927-938

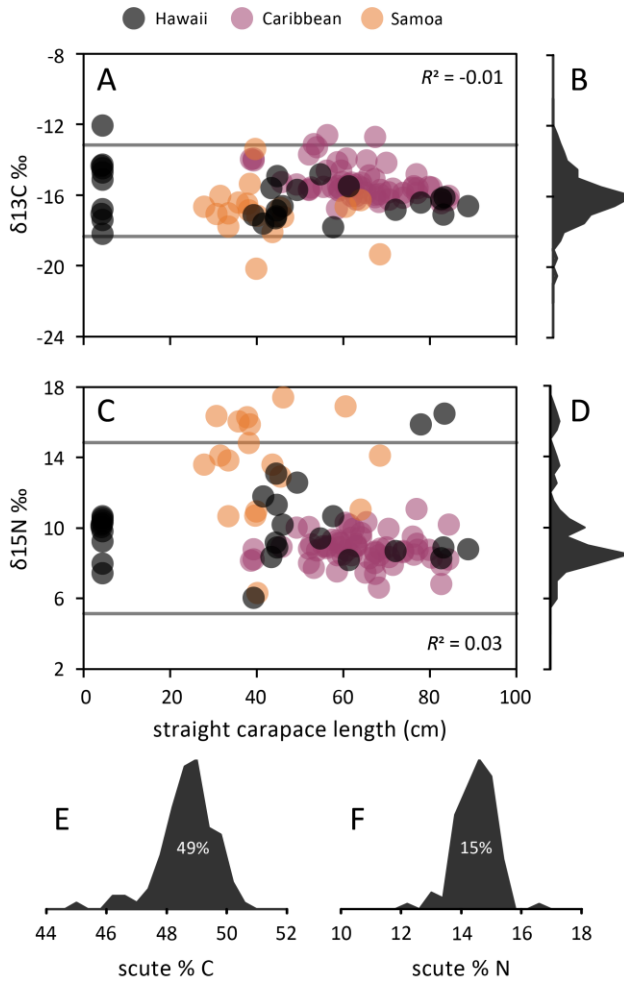
630 Wallace BP, DiMatteo AD, Hurley BJ, Finkbeiner EM, Bolten AB, Chaloupka MY, Hutchinson BJ, Abreu-Grobois FA, Amorochio D,
631 Bjorndal KA (2010) Regional management units for marine turtles: a novel framework for prioritizing conservation and research
632 across multiple scales. *Plos one* 5: e15465

633 Wedemeyer-Strombel KR, Seminoff JA, Liles MJ, Sánchez RN, Chavarría S, Valle M, Altamirano E, Gadea V, Hernandez N,
634 Peterson MJ (2021) Fishers' ecological knowledge and stable isotope analysis reveal mangrove estuaries as key developmental
635 habitats for critically endangered sea turtles. *Front Conserv Sci*: 115

636 Work TM (2000) Sea turtle necropsy manual for biologists in remote refuges. National Wildlife Health Center, Hawaii Field Station

637 Work TM, Balazs GH, Rameyer RA, Morris RA (2004) Retrospective pathology survey of green turtles *Chelonia mydas* with
638 fibropapillomatosis in the Hawaiian Islands, 1993–2003. *Dis Aquat Org* 62: 163-176

639

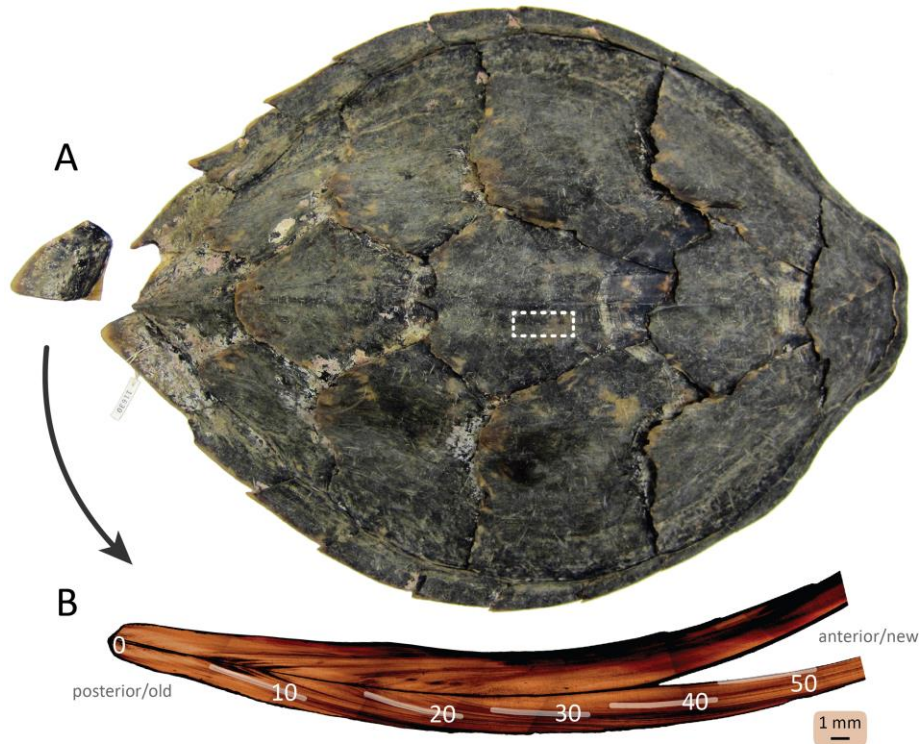


640

641

642 **Figure 1. Bulk stable isotope and elemental composition from the ventral surfaces of**
 643 **hawksbill carapace scutes.** (A) Raw results and (B) density of $\delta^{13}\text{C}$ mean values (-15.8 ± 1.32
 644 ‰), with (C) raw results and (D) density of $\delta^{15}\text{N}$ values ($10.0 \pm 2.48 \text{‰}$). Filled shapes are
 645 individual turtles comprising 10 hatchlings (4–5 cm SCL), 77 juveniles (28–71 cm SCL), and 19
 646 adults (72–89 cm SCL) from Hawaii (grey circles), Caribbean (purple squares), and American
 647 Samoa (orange triangles) populations. Horizontal grey lines are the normalized 95% interval of
 648 all 106 samples. Simple linear regressions of both series (adjusted correlation coefficients listed)
 649 show no trend through development. Density plots of (E) carbon and (F) nitrogen composition
 650 (expressed as a percentage, median values listed) indicate 36.4% of scute material is exclusive of
 651 carbon and nitrogen. Sampled tissue is from the ventral scute surfaces and captures the ecosystem
 652 experience preceding each turtle's demise. Hatchlings are ecologically naïve, and their tissues are
 653 maternally derived. As we lack samples from 8–28 cm SCL (0–4 years old) these plots do not
 654 represent the cryptic early life history phase.

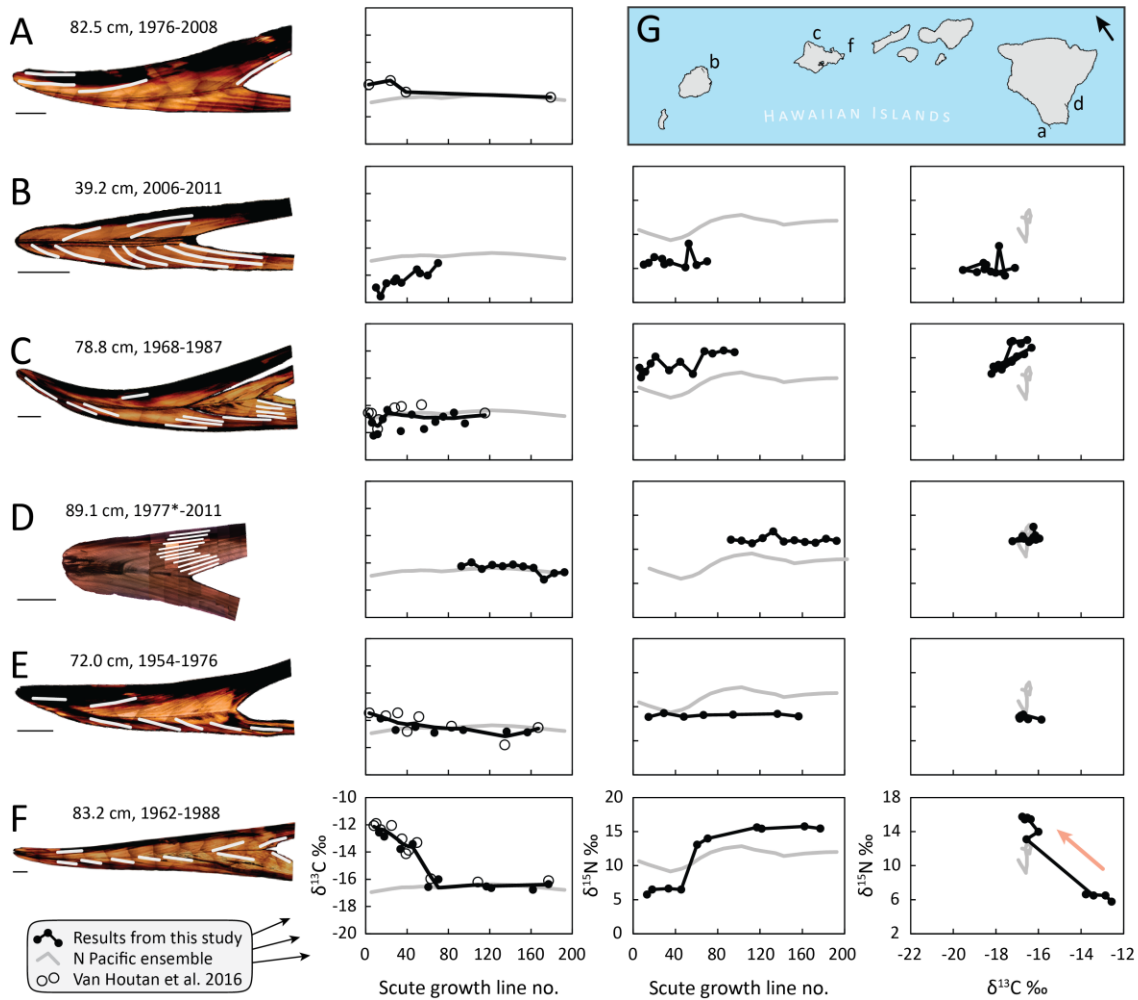
655 *Caption repeated from above for clarity*



656

657

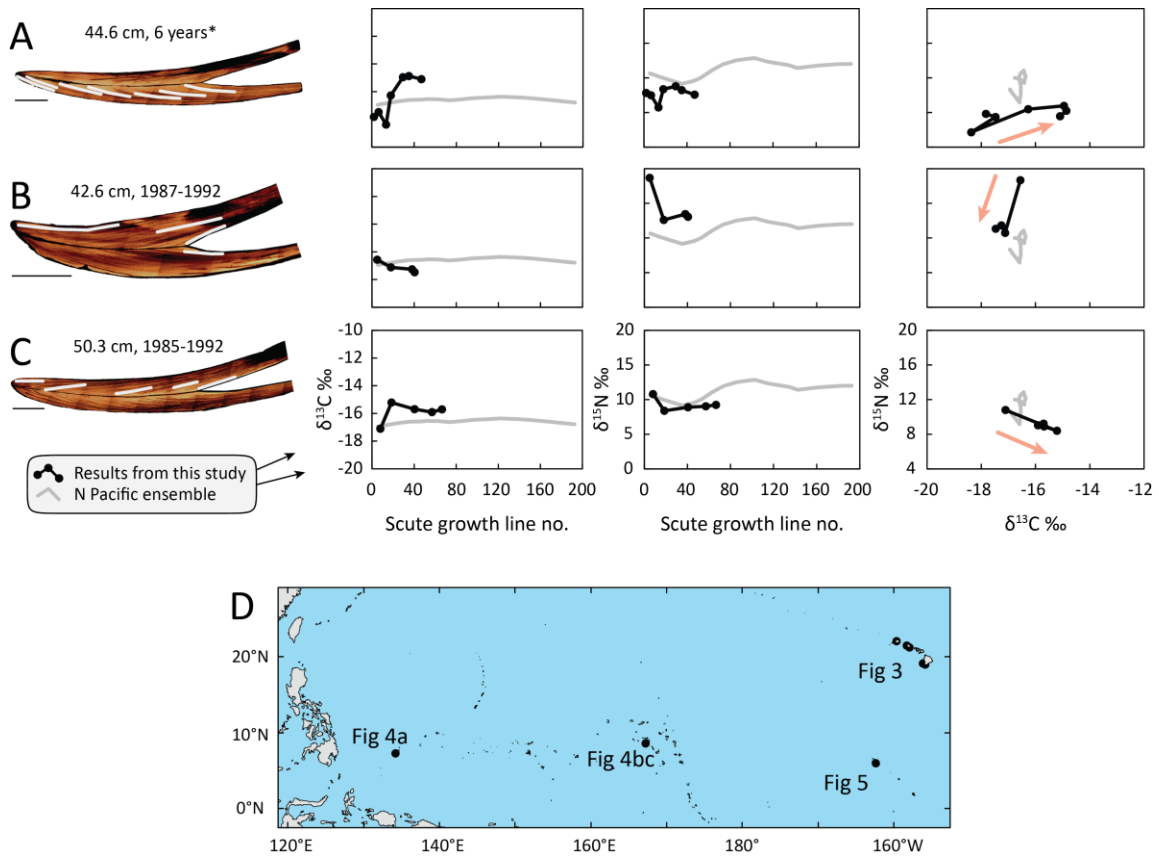
658 **Figure 2. Unlike surface material, cross sections of posterior marginal (PM) scutes from**
 659 **hawksbills contain a longitudinal chronology.** (A) Dorsal carapace view of a 44.2 cm SCL
 660 juvenile Hawaii hawkbill with the left ultimate PM removed. PM scutes both retain the largest
 661 keratin archives on the shell and can be less frequently damaged than carapace scutes. White
 662 dashed rectangle indicates the ventral surface region sampled in Figure 1. (B) PM sagittal cross
 663 section reveals a chronology of growth lines, with tissue accretion from left (posterior, old) to
 664 right (anterior, new). Cross section polished to 1-mm thickness and imaged under magnification
 665 using a combination of reflected and transmitted light. This turtle had 50 growth lines, with every
 666 tenth contour labelled and highlighted for clarity.



667

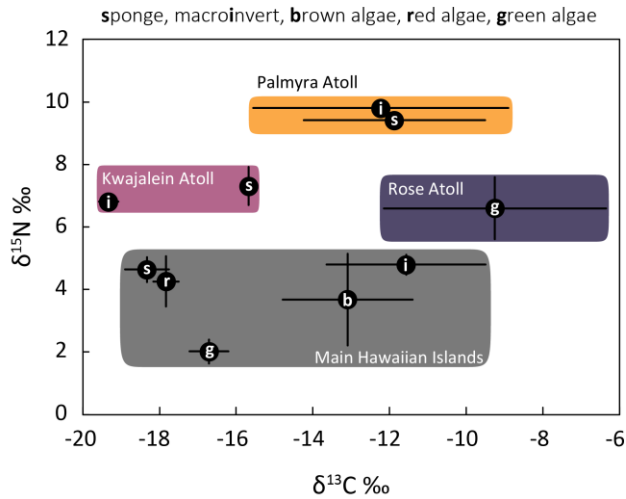
668

669 **Figure 3. Stable isotope values from scute growth contours shows several developmental**
 670 **patterns in Hawaii hawksbills.** (A–F) Imaged cross sections, drilled transects, and stable isotope
 671 results for 6 hawksbill turtles. Hollow circle $\delta^{13}\text{C}$ values and age estimates are from a previous
 672 study (Van Houtan et al. 2016a), filled circles are from the current study. Black lines interpolate
 673 values, are a LOESS when multiple data sources are available, and grey line is the ensemble
 674 average for all individuals (Figs. 3–4). From left to right (A–D, F) or top to bottom (D), drill line
 675 paths increase in age. Juvenile tissue in one turtle (D) is missing from abrasion. (G) Map of the
 676 Hawaiian archipelago locates each turtle’s stranding site (E is unknown). There is no single
 677 pattern in either carbon or nitrogen isotopes across development depicted in either single or dual
 678 variable plots. (F) Apparently demonstrates a discrete habitat shift (orange arrow), reflected in
 679 $\delta^{13}\text{C}$ and $\delta^{15}\text{N}$ values, perhaps due to nearshore settlement. Gradual shifts in $\delta^{13}\text{C}$ values (A–B, E)
 680 and (E) also indicate potential habitat shifts. Scale bar is 5 mm. Asterisk (*) indicates turtle age
 681 estimated with a von Bertalanffy growth function (see Methods).



682
683

684 **Figure 4. Stable isotope values from scute growth contours of Western Pacific hawksbills.**
 685 Though the turtles from (A) Palau and (B-C) Kwajalein Atoll are all relatively young, stable
 686 isotopes document potential shifts in both habitat and forage. Symbology retained from Figure 3,
 687 scale bars are 5 mm. Asterisk (*) indicates age estimated using measured length and previously
 688 derived VBGF parameters (Van Houtan et al. 2016a) as we had no date metadata for this
 689 specimen (see Methods). Stranding dates of (B-C) allow us to estimate birth year; (A) has no
 690 stranding date. Orange arrows indicate an apparent habitat and dietary shift. (D) Map of the
 691 central and Western Pacific with all sample collection regions noted.



692

693 **Figure 5. Stable isotope values of typical hawksbill forage item groups from four Pacific**
 694 **Island regions.** Hawksbills are omnivores that forage on sponges, other macroinvertebrates, and
 695 macroalgae. Above stable isotope values are crowdsourced from the literature (Palmyra Atoll,
 696 Pacific Remote Island Areas USA), our own collection efforts (Kwajalein Atoll, Marshall Islands;
 697 Rose Atoll, American Samoa), or a combination of both (Main Hawaiian Islands). Filled circles
 698 represent the group mean, lines are standard error. Though there is significant variability in δ¹³C
 699 values within each region, and sometimes within a single region's forage item groups, there is
 700 some structure of δ¹⁵N values between regions. These data are meant to report what currently
 701 exists, but not represent an exhaustive list of all potential hawksbill forage items in all population
 702 regions.